VII. Conclusions

A method was derived for solving a wide class of waveguide discontinuities by modal analysis. Thick and thin symmetrical H-plane bifurcations were studied. Input admittance and scattered modes were computed for a number of expansion sizes. Accuracy improved with the number of modes used.

Transverse electric-field patterns, plotted on both sides of the junction, indicated a good match for twenty and forty modes. Magnetic field matches less well due to the singularity at the vane. Even so, with forty modes the actual pattern may be easily discerned. Because permeable media do not exhibit singularities, it is believed that convergence will be much more rapid for discontinuities formed by them.

More information is required on the effects of different numbers of modes on alternate sides of a junction and on the solution's behavior as the axial length of a discontinuity vanishes.

Acknowledgment

The author wishes to acknowledge the cooperation of the University of Manitoba Computer Centre. Particular appreciation is felt for the unstinting help of K. W. Schmidt who did the programming. Dr. J. W. Bandler contributed many helpful criticisms and ideas. Much of this work was developed while the author was with International Computers and Tabulators, Ltd., London. The cooperation of their Atlas programming group is gratefully acknowledged.

References

[1] R. E. Collin, *Field Theory of Guided Waves*. New York: McGraw-Hill, 1960, pp. 409–452.
[2] L. Lewin, "On the resolution of a class of waveguide discontinuity problems by the use of singular integral equations," *IRE Trans. Microwave Theory and Techniques*, vol. MTT-9, pp. 321–332, July 1961.
[3] R. E. Collin [1], pp. 314–367.
[4] S. W. Drabowitch, "Multimode antennas," *Microwave J.*, vol. 9, pp. 41–51, January 1966.
[5] J. B. Davies and C. A. Muilwyk, "Numerical solution of uniform hollow waveguides and boundaries of arbitrary shape," *Proc. IEE* (London), vol. 113, pp. 277–284, February 1966.
[6] R. E. Collin [1], pp. 229–232.
[7] P. M. Morse and H. Feshbach, *Methods of Theoretical Physics*. New York: McGraw-Hill, 1953, pp. 928–929.
[8] C. E. Fröberg, *Introduction to Numerical Analysis*. Reading, Mass.: Addison-Wesley, 1965, pp. 172–201, 221–225.
[9] N. Marcuvitz, *Waveguide Handbook*. New York: McGraw-Hill, 1951, pp. 117–126.
[10] E. L. Ginzton, *Microwave Measurements*. New York: McGraw-Hill, 1957, pp. 317–329.
[11] C. E. Fröberg [8], pp. 74–75.
[12] N. Marcuvitz [9], pp. 172–174.

A One-GHz Ferroelectric Limiter

JOHN B. HORTON, MEMBER, IEEE, AND MERLE R. DONALDSON, SENIOR MEMBER, IEEE

Abstract—**The design and analysis of a 1-GHz limiter which uses voltage variation of the dielectric constant of a ferroelectric material to achieve limiting is described. An RF electric field derived from the input power is used to change the relative dielectric constant ε_r of the material; the resulting nonlinear change of capacitance of a small element of the material is used to change the condition of a tuned circuit. The tuned circuit terminates a quarter-wavelength stub which shunts the main transmission line, thereby providing a power-dependent mismatch at the junction of the two transmission lines. The degree of this mismatch is controlled by the condition of the tuned circuit and, therefore, the magnitude of the input power.**

Theoretical analysis and experimental results for small signal and large signal operation are presented. Limiter analysis is based on the measured change of ferroelectric (nonlinear) capacitance as a function of dc electric field. The ferroelectric element is 0.011 by 0.013 by 0.020 (inches) machined from polycrystalline ($Pb_{0.315}$–$Sr_{0.685}$) TiO_3 material.

Manuscript received November 9, 1966; revised May 10, 1967. The work reported here was performed at Sperry Microwave Electronics Co. (a Division of Sperry Rand Corp.), Clearwater, Fla., and was sponsored by the U. S. Army Electronics Command, Ft. Monmouth, N. J., under Contract DA36-039-AMC-03240(E).

J. B. Horton is with the Semiconductor Research and Development Laboratory, Texas Instruments Incorporated, Dallas, Tex. He was formerly with Sperry Microwave Electronics Company.

M. R. Donaldson is with the Electrical and Electronics Systems Department, University of South Florida, Tampa, Fla., and is a Consultant to Sperry Microwave Electronics Co.

FERROELECTRIC materials have inherent properties which cause the dielectric constant of the material to change as a function of ambient temperature and electric field. The change of dielectric constant with electric field is particularly interesting to circuit designers, since it represents a mechanism by which circuit response can be changed electrically. Applications to be considered at microwave frequencies are switches, harmonic generators, limiters, parametric amplifiers, phase shifters, etc. To date, a UHF limiter [1], an X-band harmonic generator [2], a UHF phase shifter [3], and an L-band switch [4], [5] have been reported, and parametric amplifiers have been investigated quite thoroughly [6]. The L-band passive limiter described here is a result of further effort to apply

ferroelectric material to microwave devices and in many ways complements the work reported earlier by Amoss *et al.* [5]. It is noted, however, that the mechanism being employed in the passive limiter is the nonlinear response of the ferroelectric material to RF electric field, whereas the switch designs reported by Amoss *et al.* [5], are based on the small-signal linear response of the material during suddenly applied dc electric field.

The circuit configuration used in the passive limiter design is shown in Fig. 1. The ferroelectric element is a part of the tuned circuit which is one quarter-wavelength from the main transmission line, and which provides the means of either tuning or detuning the circuit. A ferroelectric capacitance C_f, which is larger than the value necessary for resonating the tuned circuit, is used so that the magnitude of the mismatch will increase with increase of applied power. At some large electric field C_f will resonate with the inductive line and the mismatch will be a maximum. Further increase of power will cause the mismatch to decrease as the circuit again becomes detuned.

Since the insertion loss of the main transmission line is a function of mismatch on the line, the tuned circuit and quarter-wavelength stub line offer a means of producing attenuation, the magnitude of which is controlled by the applied power. This is the circuit response that is characteristic of a passive power limiter and represents the desired result here.

Analysis of the limiter circuitry is straightforward for the small signal case, where the nonlinear ferroelectric element can be approximated by a linear element. The magnitude of small signal insertion loss is from (3) (see Appendix)

$$\text{Insertion loss} - (\text{dB})\big]_{P_i \to 0} = 10 \log \frac{P_i}{P_t} = 10 \log A_0,$$

where the dependence of A_0 on circuit parameters is shown in (5).

Although the small-signal expression is not valid for the large-signal case, it may be used to estimate the qualitative performance of the circuit. Quantitative values for the limiter performance must be obtained from measurements and analysis by nonlinear methods. Both techniques were employed. The analytical procedure employed an iterative method which is summarized in the Appendix.

The choice of $(Pb_{0.315}–Sr_{0.685})TiO_3$, lead–strontium–titanate, for the ferroelectric element was made because of the low loss tangent ($\tan \delta = 0.05$), and because the Curie temperature of this combination allows room temperature (23°C) operation in the paraelectric region just above the Curie temperature. In this region, the characteristic hysteresis effects of ferroelectric materials do not exist, and the greatest change in dielectric constant for a given electric field is realized. Encapsulation details are shown in Fig. 4.4-31 by Horton and Donaldson [7]. The ferroelectric element is 0.011 by 0.013 by 0.020 (inches), with the RF field along the 0.020 dimension, and has a static nonlinear response as shown in Fig. 2. RF contact between the top of package and the ferroelectric element was made with tightly rolled aluminum foil which acted as a spring. This type of contact substantially reduced the series inductance of the package, and thereby improved the limiter characteristics.

Construction details of the limiter circuit are shown in Fig. 3. Arrangement for applying a dc bias was included to facilitate tuning for maximum isolation at a given bias voltage; adjustment of the tuning screw (C_{in}) is necessary to obtain minimum insertion loss at zero bias. Initial adjustments were made using small signals and a bias of 500 V dc; circuit Q was set at 40 to provide a circuit sensitive to small responses of the material. For the limiter application considered here, an RF electric field is used to effect the change in dielectric constant; however, as power to the element is raised to increase the RF electric field strength, thermal effects will dominate the limiter response if the loss tangent of the material is large. This is the case for materials currently available. To minimize thermal response, pulsed RF electric fields generated at very low repetition rates were used which allowed insufficient time for the relatively slow thermal effect to become an appreciable part of the overall limiter response. Electric field effects were separated from the thermal effects by using measurements on the leading edge of the output pulse. From experimental data, it was found that thermal effects were minimized if the input CW power was less than 30 mW and the ambient temperature was held at approximately 23°C.

The first test to show limiting due to RF electric field was made with constant average input power and varying duty factor. Duty factor, DF, is defined as the ratio of τ_p to T_p, where τ_p is the pulsewidth and T_p is the time between pulses. Peak power P_{pk} is defined as the ratio of P_{av} to DF where P_{av} is the average power. For given P_{av}, thermal effects should remain constant as the duty factor is decreased, and effects due to electric field should increase. Fig. 4 shows the results of this test. The lower curve ($DF = 0.82 \times 10^{-3}$) represents limiting almost totally due to thermal effects and is used to indicate thermal response present in the other curves. The peak power of the pulses for the curve of the lowest duty factor ($DF = 0.027 \times 10^{-3}$) is 30 times larger than that for the reference curve, and the additional insertion loss is attributed to the change of nonlinear capacitance due to an RF electric field.

Fig. 5 shows the input, output, and reflected pulse waveforms for 600 watts peak power input, which is a level providing approximately 5-dB limiting.

Further studies of the input and output waveforms, using pulse lengths of 0.50, 0.60, and 0.96 microsecond, illustrated the thermal effects associated with the length of test pulse. Fig. 6 shows the results for a 0.96 microsecond pulse for 230 watts peak power input. By assuming that negligible thermal limiting takes place at the leading edge of the pulse, limiting due to increase of sample temperature was found

to be 0.6, 1.0, and 2.4 dB for the three pulselengths, respectively, as measured at the output port. From these observations, the leading edge of the pulse was selected as the reference point for measuring insertion loss attributed to RF electric field.

Since the ferroelectric element is extremely sensitive to temperature, another test was made to show the limiter response to an RF electric field. A small pulse of approximately 10 watts peak power was applied to the limiter approximately two microseconds after a 700 watt pulse. Fig. 7 shows the two pulses at the input and output of the limiter. Note that the ratio of large to small pulses at the output has decreased. If thermal limiting were the only limiting present, this ratio would not decrease at the output.

When optimumly adjusted, the ferroelectric limiter has the limiting characteristic shown in Fig. 8. The small signal insertion loss is approximately 3.6 dB, and limiting occurs at approximately 200 watts input peak power with only a small change of output power up to 800 watts input. The decrease in output power is probably due to the onset of thermal effects, since the average power is 16 mW at 600 watts peak power input.

Data calculated from the expressions derived in the Appendix for output versus input power are shown in Fig. 8 with experimental data. The calculated results are based on an iterative process and agree quite well with observed data. The basic assumptions in applying the process are that the input is a sine wave of only one frequency, and that the response of the ferroelectric material to an RF electric field is that shown in Fig. 2.

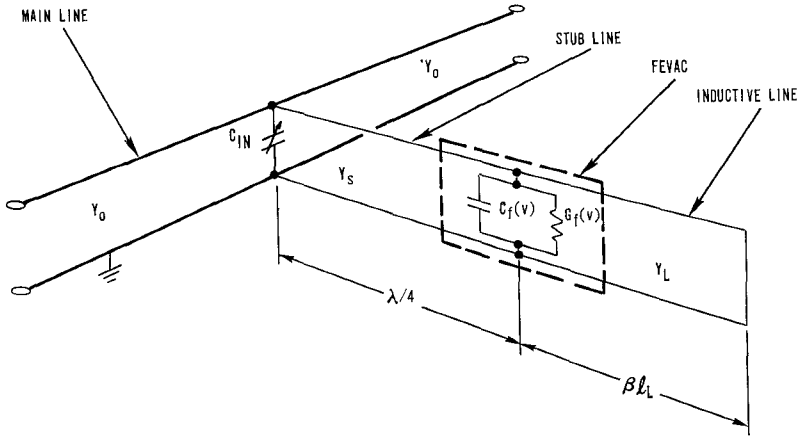

Fig. 1. Schematic diagram of a power limiter which uses a ferroelectric element.

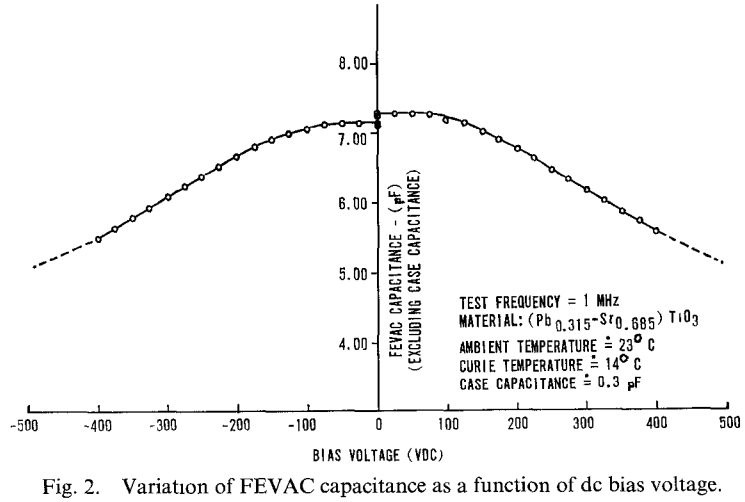

Fig. 2. Variation of FEVAC capacitance as a function of dc bias voltage.

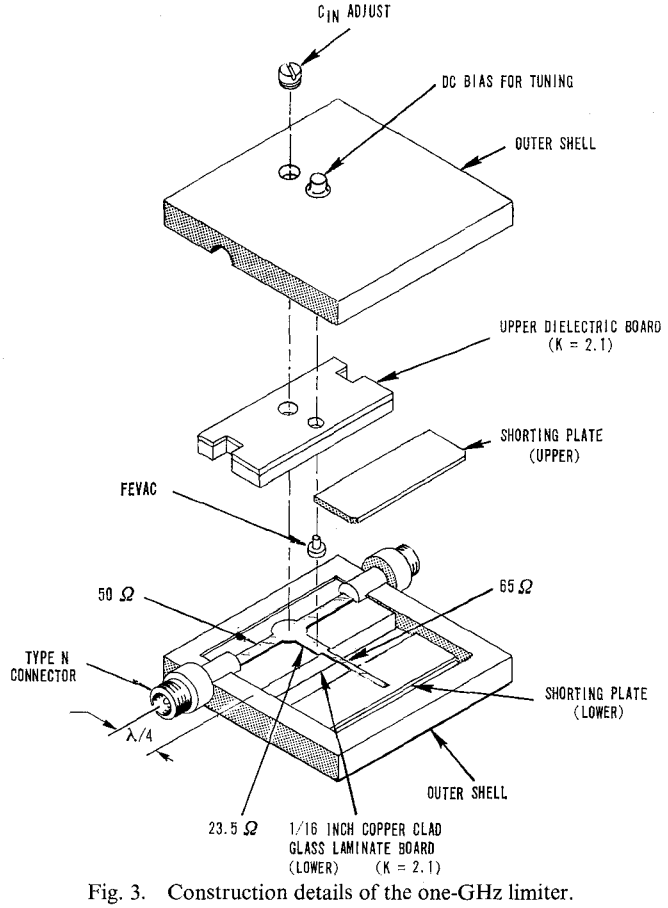

Fig. 3. Construction details of the one-GHz limiter.

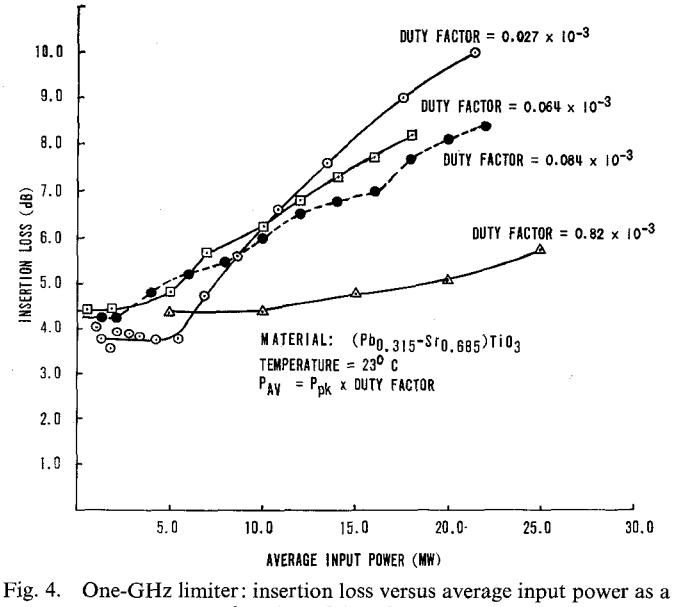

Fig. 4. One-GHz limiter: insertion loss versus average input power as a function of duty factor.

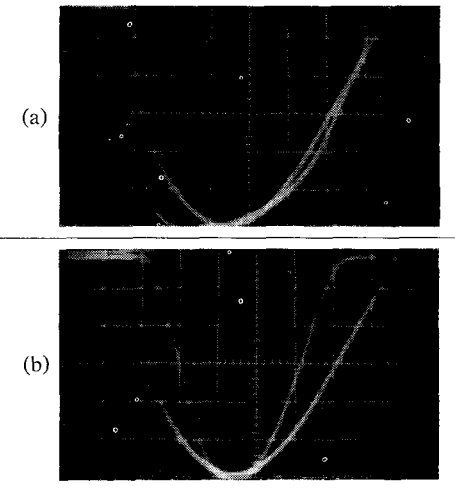

Fig. 5. One-GHz limiter: input, output, and reflected pulse waveforms for 600 watts peak power input. (a) 0.1 μs/division→. Input and output pulse waveforms. (b) 0.1 μs/division. Input and reflected waveforms.

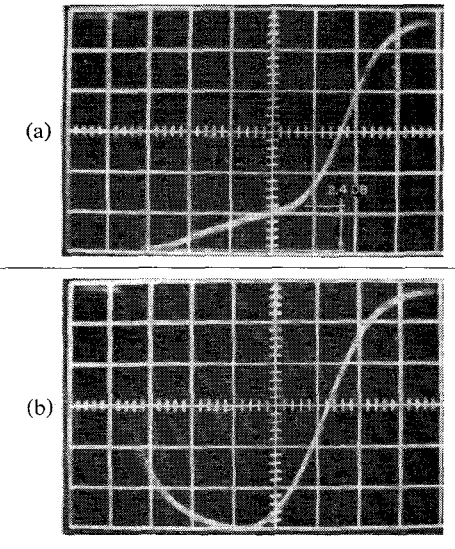

Fig. 6. One-GHz limiter: input and output pulse waveforms for 230 watts peak power input. (a) 0.2 μs/cm→. Output pulse waveform. (b) 0.2 μs/cm→. Input pulse waveform (1.0 μs).

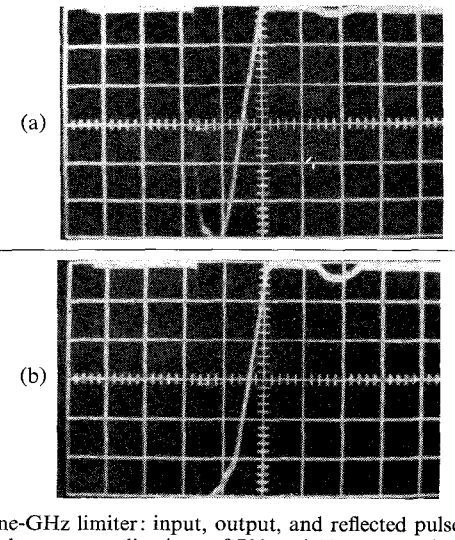

Fig. 7. One-GHz limiter: input, output, and reflected pulse waveforms for simultaneous applications of 700 and 10 watts peak power input. (a) 0.5 μs/division→. Large and small signal input pulse waveforms. (b) 0.5 μs/division→. Large and small signal output pulse waveforms.

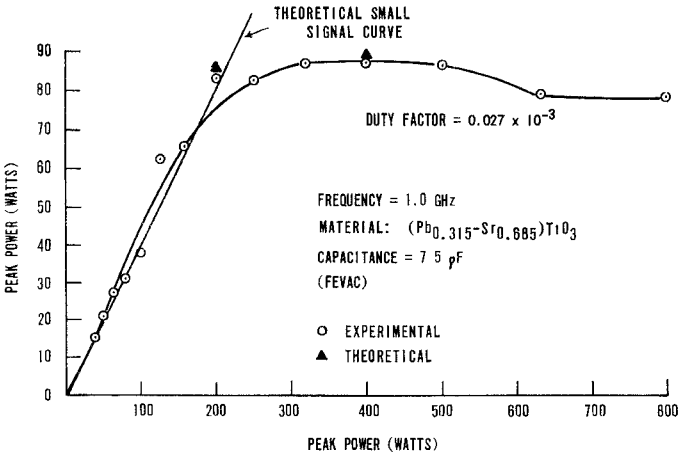

Fig. 8. One-GHz limiter: output peak power versus input peak power for duty factor $= 0.027 \times 10^{-3}$.

Conclusion

Use of the input RF electric field to effect a change of dielectric constant in a ferroelectric material is feasible, and this mechanism has been employed in a one-GHz passive limiter. Theoretical analysis of the limiter circuit, based on information obtained from the static electric field versus capacitance characteristic of the ferroelectric element, is in agreement with observations.

Results of tests on the limiter show that it responds to an RF electric field within 0.1 microsecond. However, the feorroelectric element is extremely sensitive to temperature changes, and for this reason the ferroelectric limiter will probably continue to be a laboratory device. It remains that successful design and use of a practical ferroelectric limiter for use at microwave frequencies of one GHz and above depends upon the success of reducing the thermal response of the ferroelectric material. From the point of view of material parameters, this means the loss tangent (tan δ) must be decreased in the region just beyond the Curie tempeature where the largest change of dielectric constant for an applied electric field is realized. Further considerations can be given toward improving the heat transfer from the material.

Appendix

The circuit shown in Fig. 1 is analyzed in terms of its performance to $e^{j\omega t}$ sources as a passive limiter.

Due to the presence of the voltage-dependent capacitor (FEVAC), the circuit is nonlinear. An iterative process [8] is employed to obtain a quantitative relationship between output power (P_t) and incident power at the input (P_i) of the limiter.

The main line and the stub line may be represented as a Thevenin source at the terminals of the FEVAC.

The ratio of the power dissipated in the load to the incident power at the input of the limiter can be shown to be

$$\frac{P_t}{P_i} = 4\left(\frac{Z_s^2}{Z_0}\right)^2 \left|\frac{I}{V}\right|^2, \tag{1}$$

where

$$Z_s = \frac{1}{Y_s}$$

$$Z_0 = \frac{1}{Y_0}$$

I = the Thevenin source current

V = the Thevenin source voltage.

Since the ferroelectric element is nonlinear,

$$P_t = A_0 P_i + A_1 P_i^2 + A_2 P_i^3 + \cdots. \tag{2}$$

For low signal level, the circuit is linear and

$$P_t \cong A_0 P_i. \tag{3}$$

From Fig. 1,

$$I = Z + \frac{V}{\dfrac{1}{G_0 + jB_1}} \tag{4}$$

and

$$A_0 = \frac{P_t}{P_i} = 4\left(\frac{Z_s^2}{Z_0}\right)^2 \left| \frac{1}{Z + \dfrac{1}{G_0 + jB_1}} \right|^2. \tag{5}$$

Table I lists the measured parameters of the limiter from which A_0 is computed.

$$A_0 = 4\left(\frac{552}{50}\right)^2 \cdot \left| \frac{1}{(23.5)^2\left(\dfrac{2}{50} + j0.121\right) + \dfrac{1}{0.0025 + j0.045}} \right|^2 = 0.433 \tag{6}$$

TABLE I

LIMITER PARAMETERS

$\omega_0 = 6.28 \times 10^9$ rad/s
$C_{in} = 19.3$ pF
$C_f(0) \equiv C_0 = 7.8$ pF (FEVAC capacitance at zero bias)
$Z_0 = 50$ ohms
$Z_s = 23.5$ ohms
$\tan \delta = 0.05$
$B_{in} = \omega_0 C_{in} = 0.121$ mho
$B_0 = \omega_0 C_0 = 0.049$ mho
$G_f(0) \equiv G_0 = B_0 \tan \delta = 0.0025$ mho
$B_L = \omega_0 L = 0.0345$ mho
$B_1 \equiv B_0 - B_L = 0.0145$ mho

TABLE II

ITERATIVE VALUES FOR I

$P_i = 200$ watts, $\omega = \omega_0$			$P_i = 400$ watts, $\omega = \omega_0$	
n	$\lvert V_2^{(n)} \rvert$	$\lvert I^{(n)} \rvert$	$\lvert V_2^{(n)} \rvert$	$\lvert I^{(n)} \rvert$
1	91.5	1.24	129.0	1.75
2	173.5	1.94	245.5	2.76
3	220.0	2.62	314.0	2.87
4	266.0	2.83	318.0	2.86
5	275.0	2.82		
6	238.0	2.70	P_t 90 watts	
7	241.5	2.73		
8	243.0	2.77		
P_t 84.3 watts				

from which the small signal insertion loss is

$$\text{Insertion loss}_{P_i \to 0} = 10 \log \frac{1}{0.433} = 3.63 \text{ dB}. \tag{7}$$

For the nonlinear region, a value of P_i is assumed. The Thevenin source voltage can be shown to be

$$|V| = \left| \frac{Z_s}{Z_0} \right| |E_g| = \left| \frac{Z_s}{Z_0} \right| \sqrt{4 Z_0 P_i}. \tag{8}$$

The remaining steps in the nonlinear analysis method involve choosing a value of P_i, obtaining the Thevenin voltage V corresponding to P_i by (8), and then computing I corresponding to V by iteration.

The iterative process is started by computing the voltage at ω_0 across the nonlinear element, using the Thevenin source voltage obtained from the assumed value of incident power. That is,

$$V_2 = V \frac{Z_F}{Z_F + Z}, \tag{9}$$

where

$$Z_F = \frac{1}{G_f(0) + j\omega_0 C_f(0) - j \dfrac{1}{\omega_0 L}} \tag{10}$$

is the impedance terminating the stub line at ω_0 and with zero bias applied to the nonlinear element.

With values from Table I and (8), (9) becomes

$$V_2 = 6.43 \sqrt{P_i} \lfloor -17.10^\circ. \tag{11}$$

The voltage given by (11) represents the first approximation to the voltage across the nonlinear element. The current to the FEVAC and inductive stub for this condition is

$$i(t) = i_{cf}(t) + i_{Gf}(t) + i_L = \frac{dC_f(v_2)v_2(t)}{dt} + G_f(v_2)v_2(t) + \frac{1}{L} \int v_2(t)\, dt. \tag{12}$$

The voltage dependence of $C_f(v_2)$ is assumed to be

$$C_f(v_2) = C_f(0)[1 - (kv_2)]^2, \tag{13}$$

where, from Fig. 4, k^2 is taken as

$$k^2 \cong 1.5 \times 10^{-6}. \tag{14}$$

From (13) and (14),

$$i(t) = C_f(0)[1 - 3(kv_2)^2] \frac{dv_2(t)}{dt} + G_f(v_2)v_2(t) + \frac{1}{L} \int v_2(t)\, dt. \tag{15}$$

The first approximation $i^{(1)}(t)$ to the current $i(t)$ is obtained by using $|V_2|$ from (11),

$$v_2^{(1)}(t) = 6.43 \sqrt{P_i} \cos \omega_0 t. \tag{16}$$

A second approximation to the voltage across the nonlinear element is determined by

$$v_2^{(2)}(t) = v(t) - Ri^{(1)}(t) - L \frac{di^{(1)}}{dt}(t). \tag{17}$$

The successive approximations to $i(t)$ are then calculated from (15) and (17), until the change in values of $i(t)$ on successive iterations becomes small.

The above procedure was used to compute the data shown in Fig. 8. Table II illustrates the successive values of $i^{(n)}(t)$ from the iterative process corresponding to $P_i = 200$ and 400 watts.

ACKNOWLEDGMENT

The authors wish to acknowledge the support and suggestions contributed by J. Carter and S. Dixon of USAECOM and Dr. G. R. Harrison of Sperry Microwave Electronics Co. The authors also wish to express their appreciation to B. Brown for his assistance in working on laboratory measurements.

References

[1] M. Cohn and A. F. Eikenberg, "A high-power ferroelectric limiter," *IEEE Trans. Microwave Theory and Techniques*, vol. MTT-13, pp. 47–54, January 1965.

[2] M. DiMeneico, D. A. Johnson, and R. H. Pantell, "Ferroelectric harmonic generator and the large signal microwave characteristics of a ferroelectric ceramic," *J. Appl. Phys.*, vol. 33, pp. 1697–1706, May 1962.

[3] M. Cohn and A. F. Eikenberg, "Ferroelectric phase shifters for VHF and UHF," *IRE Trans. Microwave Theory and Techniques*, vol. MTT-10, pp. 536–548, November 1962.

[4] M. R. Donaldson and L. J. Lavedan, "Microwave ferroelectric phase shifters and switches," Final Rept., U. S. Army Electronics Command, Contract DA 36-039-AMC-02340(E), March 1965.

[5] J. W. Amoss, M. R. Donaldson, L. J. Lavedan, A. L. Stanford, and J. E. Pippin, "A ferroelectric microwave switch," *IEEE Trans. Microwave Theory and Techniques*, vol. MTT-13, pp. 789–793, November 1965.

[6] S. N. Das, "Application of barium titanate compositions to parametric amplification," *IEEE Trans. Microwave Theory and Techniques (Correspondence)*, MTT-13, pp. 245–247, March 1965.

[7] J. B. Horton and M. R. Donaldson, "Investigation of large signal microwave effects in ferroelectric materials," Final Rept., U. S. Army Electronics Command, Contract DA 36-039-AMC-03240(E), March 1966.

[8] W. L. Hughes, *Nonlinear Electrical Networks*. New York: Ronald Press, 1960, ch. 5.

Correspondence

Two Partially Filled Cavity-Resonator Techniques for the Evaluation of Scalar Permittivity and Permeability of Ferrites

The two cavity-resonator techniques described earlier for measuring pure dielectrics, one using rod samples in the cylindrical cavity system,[1] and the other using slabs in a rectangular cavity system,[2] have been extended for measuring magnetic dielectrics such as ferrites. As there are four parameters that need to be evaluated, i.e., ε_r, μ_r $\tan_e \delta$, and $\tan_m \delta$; four independent measurements, two of the wavelengths in the partially filled portion, and two of the Q are needed. These two sets of measurements may either be obtained by using two different samples as in Srivastava's method,[3] or by using only one sample and obtaining the second set of measurements at a slightly different frequency (2 to 5 percent difference) and assuming that both μ and ε remain unaltered at this frequency. Since the cavities used in these methods are tunable, the second alternative, giving the unique advantage of using only one sample, is available.

Theory

Evaluation of ε_r and μ_r

ε_r and μ_r are obtained by measuring the two guide wavelengths in the partially filled portion by using Feenberg's method as explained in the earlier methods[1,2] for the two configurations mentioned above. The extraction of μ_r and ε_r from these measured parameters are given below.

Manuscript received May 18, 1966; revised May 3, 1967.

[1] J. K. Sinha and J. Brown, "A new cavity method for measuring permittivity," *Proc IEE* (London), vol. 107, Paper 3316E, November 1960.

[2] J. K. Sinha, "Modified technique for measuring dielectric constants using a rectangular cavity resonator," *IEEE Trans. Instrumentation and Measurements*, vol IM-16, pp. 32–48, March 1967.

[3] C. M. Srivastava and J. Roberts, "Measurement of ferrite loss-factors at 10 Gc/s," *Proc. IEE* (London), vol. 105, Paper 2518R, March 1958.

1) *Coaxial rod in a cylindrical cavity:* Maxwell's equations for this system give[1,4]

$$\beta^2 = \beta_0^2 - K_2^2 \tag{1}$$

$$= \beta_0^2 \mu_r \varepsilon_r - K_1^2 \tag{2}$$

and

$$\phi(x) = \frac{1}{\mu_r} \psi(y), \tag{3}$$

where

$$\phi(x) = \frac{1}{x} \frac{J_1(x)}{J_0(x)} \tag{4}$$

and

$$\psi(y) = \frac{1}{Y} \frac{J_1(y)Y_1(my) - J_1(my)Y_1(y)}{J_0(y)Y_1(my) - J_1(my)Y_0(y)}. \tag{5}$$

In the above equations, $m = r_2/r_1$, $x = K_1 r_1$, and $y = K_2 r_1$, where r_1 and r_2 are the respective radii of the specimen and the cavity.

β and β_0 in the above equations refer to the propagation constants in the partially filled portion and in the free space, respectively.

Consider the equations that would be obtained for the second set of measurements, either for the same sample at a different frequency or for a different sample at the same or different frequency. By suitable manipulation one obtains

$$K_1'^2 \beta_0^2 = K_1^2 + (K_2'^2 \beta_0^2 - K_2^2)/\beta_0'^2 \tag{6}$$

and

$$\frac{\phi(K_1)}{\phi(K_1')} = \frac{\psi(K_2)}{\psi(K_2')}. \tag{7}$$

The primed symbols correspond to the second configuration.

[4] L. Pincherle, "Electromagnetic waves in metal tubes filled longitudinally with two dielectrics," *Phys. Rev.*, vol. 66, pp. 118–130, September 1944.

K_2, $\psi(K_2)$, K_2' and $\psi(K_2')$ are now evaluated from the measured β and β'. Now, with the use of (6) and (7) one obtains an expression in K_1 or K_1' alone that can be solved numerically and, hence, μ_r and ε_r can subsequently be evaluated.

2) *Slab in the rectangular cavity:* the slab used can either be along the center or the sidewall of the cavity.[2] However, all the arguments and relations given for the previous configuration remain valid here also, except that the characteristic equations, (3)–(5), become different.

For the centrally loaded configuration one obtains

$$\phi_1(K_1 t) = 2d/t \cdot \frac{1}{\mu_r} \psi_1(K_2 d), \tag{8}$$

where

$$\phi_1 = \cot(K_1 t/2)/(K_1 t/2 \tag{9}$$

and

$$\psi_1 = \tan(K_2 d)/(K_2 d), \tag{10}$$

and where t is the thickness of the sample and d is the distance of the side of the sample to its nearest cavity sidewall.

For the side-loaded configuration, the corresponding characteristic equations are

$$\phi_2(K_1 t) = -\frac{1}{\mu_r} \psi_2(K_2 t), \tag{11}$$

where

$$\phi_2(K_1 t) = \tan K_1 t / K_1 t \tag{12}$$

and

$$\psi_2(K_2 t) = \tan K_2(a - t)/K_2 t, \tag{13}$$

and where t is the sample thickness and a the broad dimension of the waveguide used in the cavity resonator.

The efforts involved in computing the